Accuracy of linear temporomandibular joint measurements with cone beam computed tomography and digital cephalometric radiography

Michael L. Hilgers,[a] William C. Scarfe,[b] James P. Scheetz,[c] and Allan G. Farman[d]
Louisville, Ky

Introduction: Cone beam computed tomography (CBCT) is making headway into imaging for orthodontics. The purpose of this study was to define CBCT multi-planar reformatted projections for temporomandibular joint (TMJ) examination and compare the accuracy of linear measurements of the TMJ and related structures from these projections with similar measurements made with conventional cephalograms and with the anatomic truth. **Methods:** Linear dimensions between 11 anatomical sites were measured with a digital caliper to assess the anatomic truth for 25 dry human skulls. The skulls were imaged with iCAT (Xoran Technologies, Ann Arbor, Mich/Imaging Sciences International, Hatfield, Pa) CBCT, and cephalograms were made in all 3 orthogonal planes (lateral cephalometric [LC], posteroanterior [PA], and submentovertex [SMV]) acquired with photostimulable phosphor plates. Linear measurements were made on 7 custom CBCT reconstructions and the digital cephalograms. Modality means and the natural log of the standard deviations were compared post hoc against the actual dimensions by using analysis of variance with the Dunnett *t* test. Significance was set at $P < .05$. **Results:** All CBCT measurements were accurate; however, 3 of 5 LC measurements, 4 of 5 PA measurements, and 4 of 6 SMV measurements varied significantly from the truth. Intraobserver CBCT measurements were highly reliable compared with anatomic truth and significantly more reliable than measurements made from LC, PA, and SMV images. **Conclusions:** Custom oblique multi-planar reformatted reconstructions with iCAT CBCT provide accurate and reliable linear measurements of mandibular and TMJ dimensions. (Am J Orthod Dentofacial Orthop 2005;128:803-11)

Radiographic imaging, an important diagnostic adjunct in the assessment of an orthodontic patient, occasionally includes studies of the temporomandibular joint (TMJ) before or after treatment.

Various conditions affecting the TMJ can produce skeletal deformities, malocclusions, masticatory dysfunction, or derangements of the intra-articular disc.[1] Panoramic, transcranial projections, and tomography are most commonly used in the radiographic assessment of the TMJ in orthodontic practices because of availability, ease of use, low radiation requirement, and low cost.[1-3] Although many investigators have used the panoramic radiograph to assess changes in the condyle from functional appliances[4] and orthodontics,[5,6] the inherent anatomic diversity of the TMJ articulation,[7] compounded by factors that influence 2-dimensional (2D) image presentation[8] (eg, anatomic superimposition, beam projection angle, and patient positional changes) casts doubt on the validity of these reports.

Although multi-slice computed tomography (CT) provides optimal imaging of the osseous components of the TMJ, most traditional CT scanners are large and expensive systems designed for full-body imaging and are not readily available to the orthodontist. Recently, maxillofacial cone beam CT (CBCT) has been developed specifically for the maxillofacial region.[9-11] Since the introduction in the United States of the NewTom QR DVT 9000 (Quantitative Radiology s.r.l., Verona, Italy) in 2001, several systems have been commercialized, including CB MercuRay (Hitachi Medical Corp, Chiba-ken, Japan), 3D Accuitomo-XYZ Slice View Tomograph, (J. Morita Manufacturing, Kyoto, Japan), and iCAT (Xoran Technologies, Ann Arbor, Mich/

From the University of Louisville School of Dentistry, Louisville, Ky.
[a]Orthodontic resident, Department of Orthodontic and Pediatric Dentistry.
[b]Associate professor, Department of Surgical and Hospital Dentistry.
[c]Professor, Department of Surgical and Hospital Dentistry.
[d]Professor, Department of Diagnsotic Sciences, Prosthodontics and Restorative Dentistry.
Reprint requests to: William C. Scarfe, Department of Surgical and Hospital Dentistry, University of Louisville School of Dentistry, 501 S Preston St, Louisville, KY 40292; e-mail, wcscar01@louisville.edu.
Submitted, February 2005; revised and accepted, April 2005.
0889-5406/$30.00

doi:10.1016/j.ajodo.2005.08.034

Imaging Sciences International, Hatfield, Pa). These units can be categorized according to their x-ray detection systems.[12] Most CBCT units use an image intensifier tube/charge-coupled device system, whereas the iCAT uses a flat-panel imager system. The flat-panel imager detector consists of a cesium iodide scintillator applied to an amorphous silicon thin-film transistor. Images produced with image intensifier tube/charge-coupled device systems have greater noise and must be preprocessed to reduce geometric distortions inherent in the detector configuration.[12]

CBCT can provide submillimeter spatial resolution in images of high diagnostic quality with markedly shorter scanning times (10-70 seconds) and radiation dosages much smaller than traditional CT imaging methods.[13-15] Time and dose requirements are similar to other dental radiographic modalities.[16,17] CBCT allows PC-based 2D multi-planar reformatted (MPR) and secondary reconstruction of the data, providing "real-time" display modes including oblique linear and curved MPR with transaxial cross-sectional slices.

Maxillofacial applications of CBCT imaging have been reported for oral and maxillofacial surgery[18-21] and implantology,[22-25] and 3-dimensional (3D) imaging also has potential for quantitative craniofacial assessment in orthodontics.[26-31] However, before widespread adoption of this technology, accuracy and efficacy studies are warranted.

Reports on the accuracy of maxillofacial CBCT have been sparse. Kobayashi et al[25] compared the measurement accuracy of conventional spiral CT and CBCT for assessing the alveolar ridge height of 5 mandibles. They found significant differences in measurement error between the 2 modalities (spiral CT: mean 2.2%, range 0%-6.9%; CBCT: mean 1.4%, range 0.1%-5.2%). Lascala et al[32] evaluated the accuracy of linear measurements obtained from 8 skulls imaged with a NewTom 9000. They found that the real measurements were always larger than those calculated with CBCT images, but the differences were only significantly different from the truth for the skull-base structures. Although Tsiklakis et al[33] presented 4 cases using CBCT 2D MPR projections that included TMJ examination, only 1 preliminary report concerning a prototype device specifically addressed the accuracy of TMJ dimensions.[34]

The aims of this study were to develop CBCT MPR projections to demonstrate TMJ morphology and selected mandibular relationships, and compare the reliability and accuracy of measurements derived from these images with conventional photostimulable phosphor cephalograms in 3 planes to anatomic truth.

MATERIAL AND METHODS

This study, an in-vitro prospective self-controlled unblinded experiment, was approved by the Institutional Human Remains Committee, Department of Anatomical Sciences and Neurobiology, at the University of Louisville. No demographic data were available on the human remains; the skulls were not identified by age, sex, or ethnicity. The TMJ articulations (n = 50) of 25 skulls were inspected. The condyles were essentially normal morphologically, but, because the specimens are used in teaching, some lateral and medial condylar poles showed wear. The severity and distribution of such defects were recorded photographically.

To provide some semblance of soft-tissue attenuation, 2 or 3 latex balloons filled with water were placed in the cranial vault before imaging. To simulate the TMJ interarticular space and separate the mandibular condyle from the temporal fossa, a 1.5-mm-thick foam wedge was placed in the joint space between the glenoid fossa and the condylar head. For all images, the teeth were placed in centric occlusion (maximum intercuspation), and the jaws were held closed by bilateral metal springs. A plastic head holder, with a polyvinyl chloride pipe extension for placing into the foramen magnum, was constructed to support the skulls during imaging.

Imaging

Four radiographic modalities (CBCT and 3 cephalograms) were used:

Cephalometric transmission radiography was performed by using a Quint Sectograph (Model QS 10-1627W; Denar, Anaheim, Calif) and 10:1 parallel grid. The source-to-midsagittal plane distance was maintained at 1.5 m. The detector was positioned 15 cm from the midsagittal plane for all exposures. Exposure settings were 78 kVp, 200 mA, and 2/15 seconds.

For the lateral cephalogram (LC), the skull was stabilized by 2 ear rods inserted into the external auditory meati and positioned with the Frankfort plane parallel to the floor, the sagittal plane perpendicular to the x-ray beam, and the left side closest to the detector. The central ray was directed at the right external auditory meatus.

For the posteroanterior cephalogram (PA), the skull was stabilized by 2 ear rods inserted into the external auditory meati and positioned with the Frankfort plane parallel to the floor and the sagittal plane parallel to the x-ray beam with the facial bones closest to the detector. The central ray was directed midway between the external auditory meati at the level of the external nuchal line.

Table I. Definitions of anatomic landmarks used as references for linear measurements

Landmark	*Definition (representative figure)*
Posterior mandibular condyle (PCo)	Most posterior extent of mandibular condyle located 4 mm inferior to apex of superior condylar surface
Anterior mandibular condyle (ACo)	Most anterior extent of mandibular condyle located 4 mm inferior to apex of superior condylar surface
Lateral mandibular condyle (LCo)	Most lateral extent of mandibular pole of condyle viewed coronally
Medial mandibular condyle (MCo)	Most medial extent of mandibular pole of condyle viewed coronally
Superior mandible condyle (SCo)	Most superior apex on concavity of condylar head viewed sagittally
Inferior sigmoid notch (InfSig)	Most inferior apex on concavity between coronoid and condylar process of mandible viewed sagittally
Pogonion (Pog)	Most anterior midsagittal point along convexity of chin of mandibular body viewed sagittally
Posterior superior mandibular condyle (PSCo)	Point along posterior superior surface of mandibular condyle which is greatest distance from Pog viewed sagittally
Distal second molar (DM2)	Most superior distal contact point of crown of second mandibular molar relative to Pog in sagittal plane
Mesial second molar (MM2)	Most lingual mesial contact point of crown of second mandibular molar in axial plane
Gonion (Go)	Point midway along curvature of angle of mandible between inferior border of body and posterior border of ramus of mandible viewed sagittally

For the submentovertex (SMV), the skull was stabilized by 2 ear rods inserted into the external auditory meati and positioned with the Frankfort plane perpendicular to the floor. This required the chin to be raised. In addition, the skull was oriented with the sagittal plane parallel to the x-ray beam with the front of the skull facing the x-ray beam and the vertex of the skull closest to the detector. The central ray was aimed midway between the condyles.

CBCT images were acquired with the iCAT CBCT unit. The device was operated at 1-3 mA and 120 kVcp by using a high-frequency generator with fixed anode and 0.5 mm nominal focal spot size. The anterior symphyseal region of the mandible of each skull was inserted into the chin holder, and vertical and horizontal lasers were used to position the skull. The skull was oriented by adjusting the chin support until the midsagittal plane was perpendicular to the floor and the horizontal laser reference coincided with the intersection of the posterior maxillary teeth and the alveolar ridge. Lateral scout radiographs were taken and small adjustments made so that discrepancies between bilateral structures (eg, posterior and inferior borders of the mandibular rami and zygomatic arches) were less than 5 mm.

A single 360° rotation, 20-second scan, comprising 306 basis projections, was then made for each skull with a 17.0 cm (diameter) × 13.2 cm (height) field of view by using iCAT acquisition software (version 1.7.7). Primary reconstruction of the data, automatically performed immediately after acquisition, took approximately 60 seconds. Secondary reconstruction occurs in "real time" and provides contiguous color correlated perpendicular axial, coronal, and sagittal 2D MPR slices, resulting in 330 individual 0.4-mm slices in each orthogonal plane.

The cephalograms were acquired with an 8 × 10-in photostimulable storage phosphor imaging plate scanned at 300 dpi and recorded as 16-bit TIFF by using the DenOptix imaging system (Gendex/KaVo, Lake Zurich, Ill). The proprietary software used was VixWin 2000 version 1.2 (Gendex/KaVo). Images were stored in 16-bit TIF format. For display and analysis, the cephalograms were equalized before measurement. (Equalization redistributes the pixel values so that they are distributed over the entire range of brightness levels.) CBCT images were acquired with a megapixel (1024 × 1024 matrix) flat-panel hydrogenated amorphous silicon detector with cesium iodide scintillator.

Measurement analysis

For each skull, 11 anatomic landmarks were identified and indelibly marked (Table I, Fig 1). Ten linear measurements directly characterizing the size of the condyles (width, length, and height) and representing intercondylar (maximum lateral and medial intercondylar distance), TMJ/mandible (pogonion to condyle, pogonion to distal second molar, lateral mandibular condyle to gonion), and mandibular (maximum mandibular molar and maximum mandibular width) spatial relationships were developed (Table II, Fig 1).

To establish the true distances between the selected anatomic points, 3 independent measurements were made by the first author directly using an electronic digital caliper (27-500-90, GAC, Bohemia, NY). For

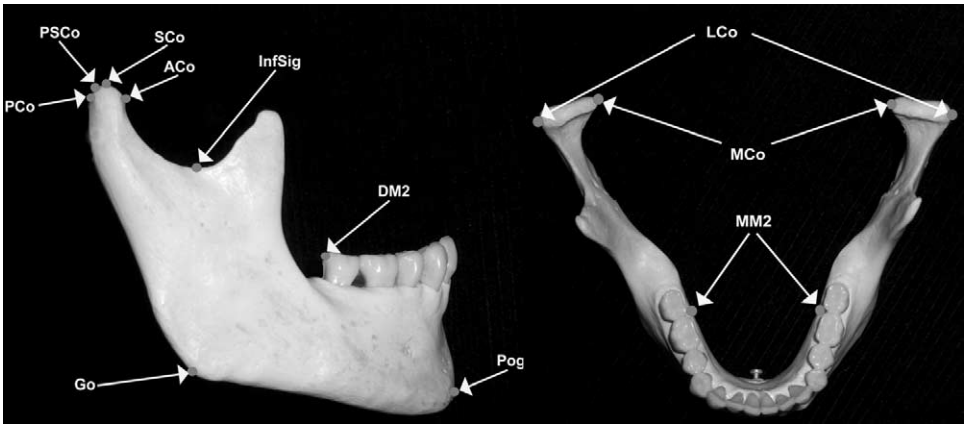

Fig 1. Lateral (*left*) and sagittal (*right*) views of mandible showing positions of anatomic landmarks.

Table II. Definitions of TMJ and mandibular linear measurements

Measurement	*Linear distance*	*Definition*
Condylar length	PCo – ACo	Linear distance between posterior mandibular condyle and anterior mandible condyle in sagittal plane
Condylar width	MCo – LCo	Linear distance between medial mandibular condyle and lateral mandible condyle in coronal plane
Condylar height	CoHt	Perpendicular linear distance from superior mandible condyle (SCo) to tangent constructed between most inferior point of coronoid sigmoid notch (InfSig) perpendicular to tangent of posterior surface of ramus in sagittal plane
Pogonion to Condyle	Pog – PSCo	Linear distance between Pog and posterior superior mandibular condyle in sagittal plane
Pogonion to distal second molar	Pog – DM2	Linear distance between Pog and most distal superior point of crown of second mandibular molar in sagittal plane
Lateral mandibular condyle to gonion	LCo – Go	Linear distance between lateral mandibular condyle and Go in coronal plane
Maximum lateral intercondylar distance	LCo – LCo	Linear distance between lateral mandibular condyles in coronal plane
Maximum medial intercondylar distance	MCo – MCo	Linear distance between medial mandibular condyles in coronal plane
Maximum mandibular molar width	M2 – M2	Linear distance between most distal superior distal contact point of second mandibular molars in coronal plane
Maximum mandibular width	Go – Go	Linear distance between gonion point in coronal plane

digital cephalogram display, the monitor was a 17-in. flat panel color thin film transistor (Pl713s; Proview, Garden View, Calif) screen with a resolution of 1280 × 1024 and a 0.264 mm dot pitch, operated at 32 bit. Equalized images were magnified 200%, and linear distances were measured by using a cursor-driven measurement algorithm. All measured distances from the cephalograms were calibrated according to the image-casting magnification factor determined for a 100-mm metal ruler placed in the midplane of the skull perpendicular to the radiographic beam. The calculated magnification reductions needed were LC = 9.92%, SMV = 9.98%, and PA = 10.21%.

Many measurements required identification of bilateral structures that are inherently difficult to view on conventional cephalometric images. Some dimensions involved the determination of points on the condyle. On LCs, it is difficult to differentiate between left and right condyles; however, rather than make an educated guess on the shape of a "hybrid" condyle developed from a visual summation of images, we attempted to distinguish condyles individually based on an assumption that the right condyle was larger (with a projection geometry and right side of the skull positioned closer to the radiation source). If the condyles could not be differentiated, both right and left condyle landmarks were considered coincident. Although theoretically this would lead to differential magnification of left- and right-sided condylar images compared with the midsagittal correction factor, the minimal influence on abso-

Table III. Description of CBCT projections used for dimensional assessments

Projection	*Image projection construction method and measurement (slice thickness in mm)*	*Linear dimension*
Limited area, transoblique, narrow slice	Axial image adjusted to image maximum mediolateral condylar dimension, oblique 2D MPR constructed along poles of condyle	PCo – ACo
Limited area, transoblique, narrow slice	Axial image adjusted to image condyle and superior tip of coronoid process, oblique 2D MPR constructed through tip of coronoid and anterior margin of external auditory meatus	MCo – LCo
Wide area, oblique, medium slice	Axial image adjusted to image condyle and superior tip of coronoid process, oblique 2D MPR (10 mm) constructed through tip of coronoid and anterior margin of external auditory meatus	CoHt
Wide area, oblique, medium slice	Axial image adjusted to image condyle and superior tip of coronoid process, oblique 2D MPR (12.4 mm) constructed through posterior margin of external auditory meatus anteriorly through pogonion by scrolling axial image	Pog – PSCo, Pog – DM2
Wide area, oblique, wide slice	Axial image adjusted to image condyle and superior tip of coronoid process, oblique 2D MPR (28 mm) constructed through anterior margin of condyle at junction of neck of condyle by scrolling axial image	LCo – Go, Go – Go
Wide area, oblique, medium slice	Axial image adjusted to image condyle and superior tip of coronoid process, oblique 2D MPR (10 mm) constructed through lateral poles of both condyles	LCo – LCo, MCo – MCo
Wide area, axial, narrow slice	Axial image adjusted to image interproximal contact between first and second mandibular molars	M2 – M2

lute dimension in relation to the size of the feature and the summation of these distances should average the effect.

For CBCT, we used a 20.1-in flat panel TFT color monitor (Flexscan L885, Eizo Nanao, Ishikawa, Japan) with a screen resolution of 1600 × 1200 and a 0.255 × 0.255 mm pixel pitch operated at 32 bit.

Because each cephalogram provides only 2D information in a single plane, a combination of 3 cephalographic projections was needed to visualize the linear dimensions selected for measurement. CBCT acquires 3D data; therefore, it is possible to provide multiple tertiary projections to derive all linear dimensions. The iCAT CBCT default display provides coronal, axial, and sagittal 0.4 mm image slices. For measurement purposes, it was necessary to develop 7 alternate projections by using the manufacturer's proprietary software. The parameters used to provide appropriate images demonstrating the defined landmarks are summarized in Table III and illustrated in Figures 2-4.

Data analysis

All data were entered into Excel 2003 (Microsoft, Redmond, Wash). Means and standard deviations of 3 independent repeats of the 10 measurements were calculated for each specimen and modality. The data files were then coded for use with the Statistical Package for the Social Sciences software (version 12.0, SPSS, Chicago, Ill). The measurement dimensions were each determined to be distributed normally, so the mean of the 3 repeat measurements was used in the analysis. Analysis of the standard deviation of the repeat measurements did not demonstrate a normal distribution; therefore, the natural log of each standard deviation was used as an index of intraobserver reliability. The statistical methods consisted of a 1-way ANOVA for each measurement dimension and the natural log of the standard deviations. The post hoc survey used the Dunnett *t* test with the actual anatomic dimensions as the control.

RESULTS

In the TMJ sample (n = 50), 24 condyles were intact, and the remaining condyles had minor defects considered to represent loss of no more than 3 mm of bone. Twenty condyles had lateral defects only, 3 had medial defects only, and 3 had bilateral defects.

Table IV lists the directly measured mean dimensions for each specimen compared with those obtained from iCAT CBCT images and digital cephalograms. No measurement made with the iCAT differed significantly from the anatomic truth. By using the LC image, 3 of the possible 5 mean linear measurements—condylar length ($P < .001$), condylar height ($P < .01$), and the lateral pole to gonion ($P < .001$)—were significantly greater than anatomic truth by 2.28 mm (25.9%) on average, 1.97 mm (10.1%) on average, and 8.99 mm (17.5%) on average, respectively. For PA measurements, 4 of the 5 mean linear measurements—condylar length ($P < .001$), lateral distance between condyles

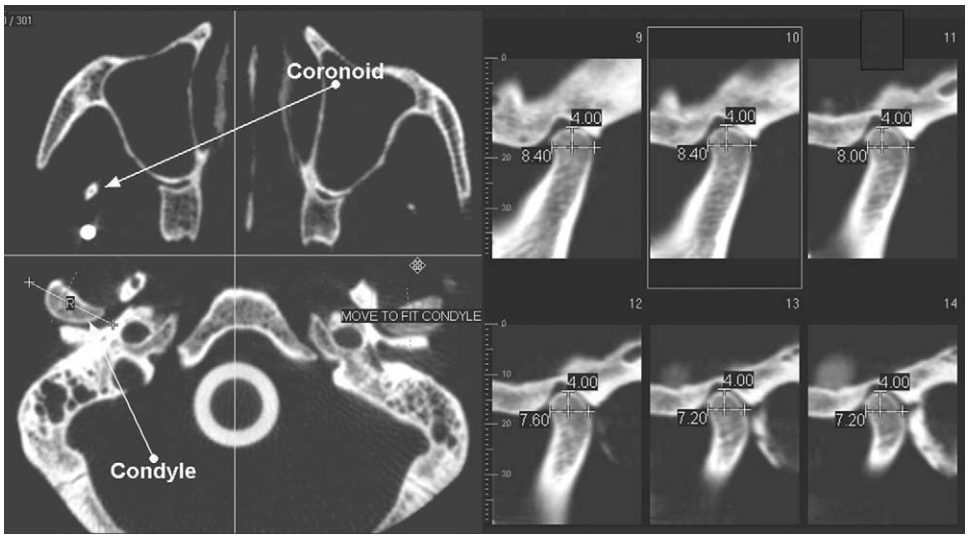

Fig 2. CBCT 2D MPR projection showing PCo – ACo. *Left*: Axial slice showing condyle and coronoid process with bilateral thin slice limited area linear oblique MPR through condylar poles. *Right*: Condylar width determined from assessment of maximum anterior posterior dimension 4 mm inferior to condylar apex on 1-mm transaxial slices. In this example, PCo – ACo = 8.4 mm. (See Table I for abbreviations.)

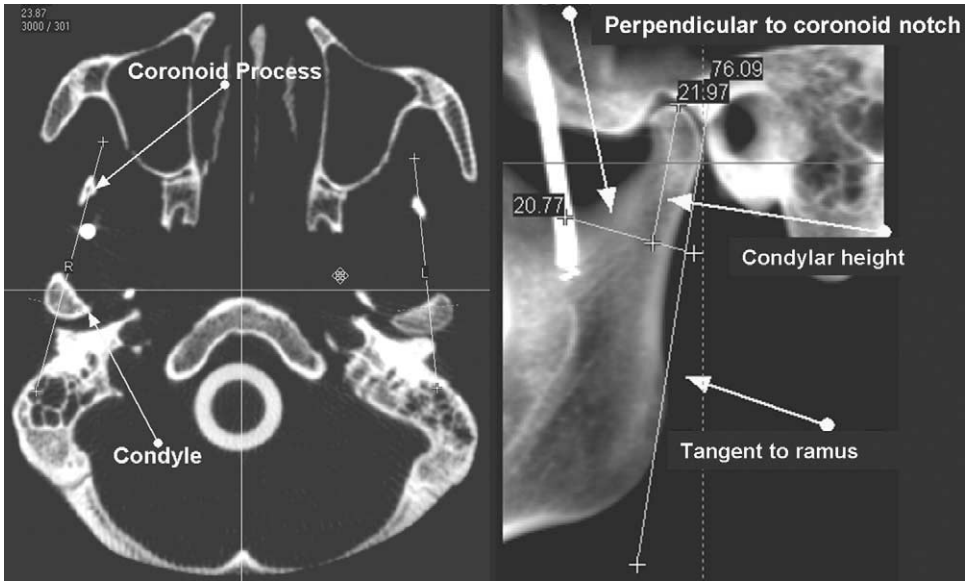

Fig 3. CBCT 2D MPR projection showing CoHt. Axial slice showing bilateral medium slice (10 mm) wide area linear oblique MPR through tip of coronoid and anterior external auditor meatus. Resultant image demonstrating construction of condylar height as a plane parallel to ramus tangent through superior apex of condyle (right). In this example, CoHt = 21.97 mm. (See Table II for abbreviation.)

($P < .001$), medial distance between condyles ($P < .001$), and gonion to gonion ($P < .05$)—were significantly greater than anatomic truth by 2.3 mm (10.8%) on average, 10.29 mm (9.4 %) on average, 7.0 mm (9.6%) on average, and 6.65 mm (7.3%) on average, respectively. Four of the 6 SMV mean linear measurements—condylar height ($P < .01$), lateral distance between condyles ($P < .001$), medial distance between

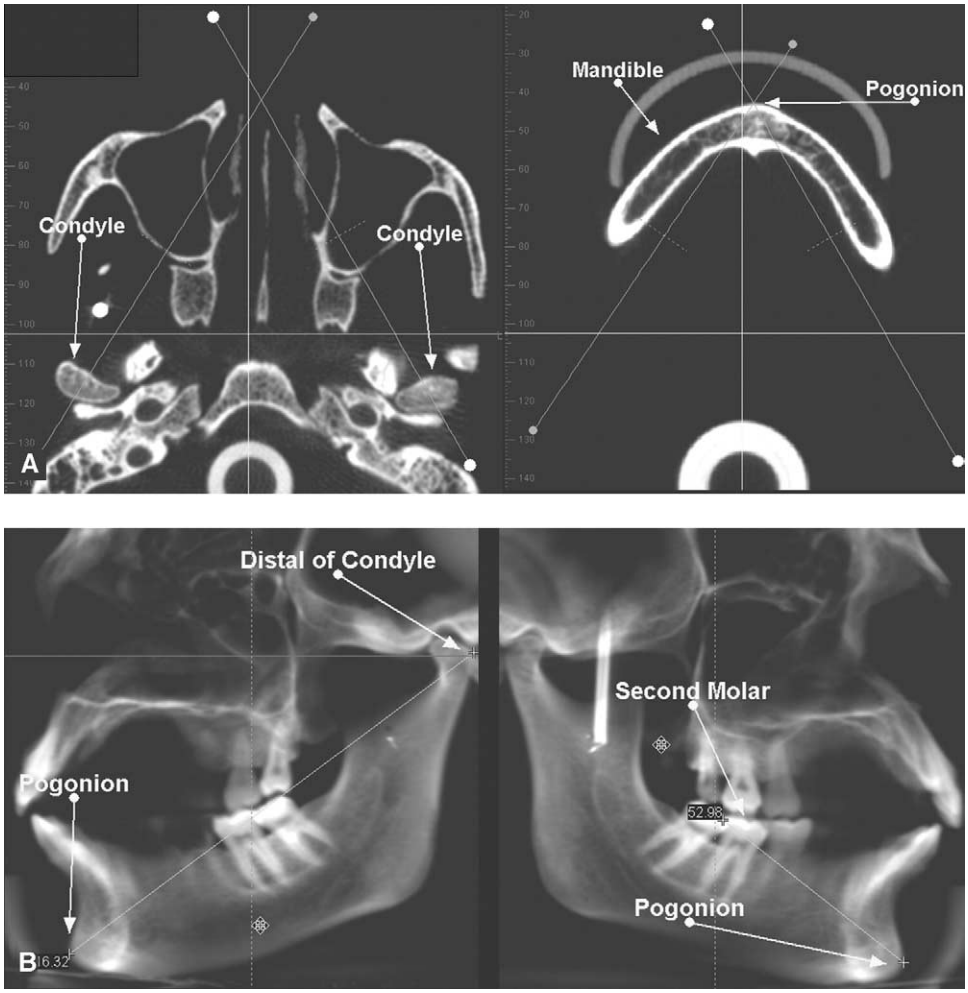

Fig 4. CBCT 2D MPR projection showing Pog – PSCo and Pog – DM2. **A**, Axial slices showing linear oblique MPR through posterior margin of external auditory meatus (*left*) and more inferior axial slice through pogonion (*right*). **B**, Medium slice (12.4 mm) wide area MPR slices showing pogonion to distal of condyle (*left*) and pogonion to distal of second molar (*right*). In this example, Pog – PSCo = 116.32 mm and Pog – DM2 = 52.98 mm. (See Table II for abbreviations.)

condyles ($P < .001$), and maximum molar width ($P < .001$)—were significantly greater than anatomic truth by 1.32 mm (7.0%) on average, 10.65 mm (9.8%) on average, 8.68 mm (11.9%) on average, and 5.67 mm (14.6%) on average, respectively.

Table V lists standard deviations for the measured anatomic truths compared with the standard deviations of measurements obtained from iCAT CBCT images and each digital cephalogram projection. Standard deviations are an index of intrarater reliability. The variability of all measurements made with the iCAT were significantly lower than those from the experimental error in direct anatomic measurement, except for the medial distance between condyles and gonion to gonion. The variability of all cephalometric measurements except for 2 LC standard deviations (pogonion to condyle and pogonion to distal second molar) was significantly greater than those due to experimental errors in measuring the anatomic truth.

DISCUSSION

There was no single imaging technique readily available to the orthodontist that provided accurate representation of all osseous aspects of the TMJ complex and associated structures until the recent commercialization of CBCT. Formerly, conventional cephalometric projections such as the LC, PA, and SMV were used individually or in combination to provide 2D representations of structures in 3 planes of space. CT has been used in TMJ evaluation; however, financial

Table IV. Comparisons of image-based mean measurements (mm) to anatomic truth

Linear dimension	*N*	*Truth*	*iCAT*	*LC*	*PA*	*SMV*
PCo – ACo	50	8.80	8.81	11.08‡		9.18
MCo – LCo	50	18.76	18.83		20.79‡	20.08†
CoHt	50	19.46	19.56	21.43†		
Pog – PSCo	50	117.10	117.52	119.33		
Pog – DM2	50	54.79	55.15	53.85		
LCo – Go	50	51.44	51.59	60.43‡	58.26	
LCo – LCo	25	109.22	109.28		119.51‡	119.87‡
MCo – MCo	25	73.13	73.13		80.13‡	81.81‡
M2 – M2	25	38.84	38.88			44.51‡
Go – Go	25	90.69	89.94		97.34*	88.35

*$P < .05$; †$P < .01$; ‡$P < .001$.

Table V. Comparisons of image-based measurement standard deviations (mm) to standard deviations from experimental errors in repeat determinations of anatomic truth

Linear dimension	*N*	*Truth*	*iCAT*	*LC*	*PA*	*SMV*
PCo – ACo	50	0.13	0.08†	0.37‡		0.28‡
MCo – LCo	50	0.03	0.10‡		0.57‡	0.32‡
CoHt	50	0.01	0.16‡	0.42‡		
Pog – PSCo	50	0.05	0.09†	0.44		
Pog – DM2	50	0.36	0.11‡	0.39		
LCo – Go	50	0.034	0.13‡	0.58‡	0.61‡	
LCo – LCo	25	0.04	0.08‡		0.64‡	0.36‡
MCo – MCo	25	0.06	0.07		0.56‡	0.25‡
M2 – M2	25	0.18	0.09†			0.49‡
Go – Go	25	0.16	0.28		0.48‡	0.38‡

†$P < .01$; ‡$P < .001$.

and radiation dose costs, as well as access, inherently limit the routine use of this modality in orthodontics. Conventional corrected TMJ tomography was not evaluated in this study because it is rarely available in an orthodontic office. In addition, although tomography provides information on the relative shape of the surfaces of the glenoid fossa and condyle, direct measurements are not usually made from the images, and no cephalometric analysis is performed by using the modality.

We found CBCT images to be remarkably accurate compared with direct anatomic measurements, whereas measurements made with conventional cephalograms were significantly greater than the anatomic truth in most instances, even after calibration. Although the consistently higher measurements with conventional radiographs could have resulted from operator error, this is unlikely because each measurement was repeated 3 times. More than likely, the difference reflects that CBCT images in a 2D plane have inherently higher contrast. This gives the observer a specific 2D plane and a structure without anatomic noise due to superimposition on which it is easier to identify landmarks. Absolute differences from anatomic truth generally were statistically significant and also considered large enough to be of clinical importance. The iCAT CBCT images were found to effect a nearly 1:1 reconstruction representation of the TMJ complex in all dimensions.

Studies of conventional CT have indicated that measurement error in craniofacial imaging within 5% is clinically acceptable.[35] Lascala et al[32] reported that CBCT imaging accuracy was statistically insignificantly different from anatomic truth for maxillary measurements, but that measurements with an image intensifier tube/charge-coupled device CBCT (Newtom, Verona, Italy) were significantly larger than the anatomic truth for the skull base. Beason and Brooks[34] presented pilot data evaluating the accuracy of measurements made on 26 condyles with DentoCAT (prototype iCAT) images compared with direct measurements of the actual specimens. They found that measurements made from 2D image reconstruction were significantly smaller than the measured truth and proposed that this difference could be due to inaccurate calibration of the reconstruction program. Our results suggest that iCAT now provides greater accuracy. In a typical orthodontic practice, practitioners do not take into account magnification differences between right and left TMJs on a lateral cephalometric image. Therefore, measurements from a CBCT image could be more accurate because practitioners can make them without introducing magnification effects.

Further research on the application of CBCT imaging to orthodontics is indicated. The level of accuracy and reliability afforded by CBCT should facilitate the measurement of parameters affected by orthodontic or orthopedic intervention including effects of occlusal alteration, surgery, and appliance therapy on the TMJ. Three-dimensional imaging has long been proposed as the ideal cephalometric image, but the user interface and computational requirements associated with either surface- or volume-rendered data have been limited. Emerging CBCT projections such as maximum intensity profile could facilitate topographic analysis.

CONCLUSIONS

iCAT CBCT accurately depicts the TMJ complex in 3D. Measurements were reproducible and significantly more accurate than those made with conventional cephalograms in all 3 orthogonal planes.

We thank Dr Anibal Silveira, Department of Orthodontic and Pediatric Dentistry, University of Louisville, for his constructive comments during this project.

REFERENCES

1. Brooks SL, Brand JW, Gibbs SJ, Hollender L, Lurie AG, Omnell KA, et al. Imaging of the temporomandibular joint: a position paper of the American Academy of Oral and Maxillofacial Radiology. Oral Surg Oral Med Oral Pathol Oral Radiol Endod 1997;83:609-18.
2. Katzberg RW. State of the art: temporomandibular joint imaging. Ann Roy Aust Coll Dent Surg 1989;10:2-52.
3. Dixon D. Radiographic diagnosis of temporomandibular disorders. In: Sadowsky PL, Laskin DM, editors. Seminars in orthodontics: temporomandibular joint disorders: fact or fiction. Philadelphia: W. B. Saunders; 1995. p. 207-21.
4. Uematsu H, Ichida T, Masumi S, Morimoto Y, Tanaka T, Konoo T, et al. Diagnostic image analyses of activator treated temporomandibular joint in growth and maturing stages. Cranio 2002; 20:254-63.
5. Peltola JS, Kononen M, Nystrom M. A follow-up study of radiographic findings in the mandibular condyles of orthodontically treated patients and associations with TMD. J Dent Res 1995;74:1571-6.
6. Carlton KL, Nanda RS. Prospective study of posttreatment changes in the temporomandibular joint. Am J Orthod Dentofacial Orthop 2002;122:486-90.
7. Solberg WK, Hansson TL, Nordstrom B. The temporomandibular joint in young adults at autopsy: a morphologic classification and evaluation. J Oral Rehabil 1985;12:303-21.
8. McDavid WD, Tronje G, Welander U, Morris CR. Dimensional reproduction in rotational panoramic radiography. Oral Surg Oral Med Oral Pathol 1986;62:96-101.
9. Mozzo P, Procacci C, Tacconi A, Martini PT, Andreis IA. A new volumetric CT machine for dental imaging based on the cone-beam technique: preliminary results. Eur Radiol 1998;8:1558-64.
10. Hashimoto K, Arai Y, Iwai K, Araki M, Kawashima S, Terakado M. A comparison of a new limited cone beam computed tomography machine for dental use with a multidetector row helical CT machine. Oral Surg Oral Med Oral Pathol Oral Radiol Endod 2003;95:371-7.
11. Sukovic P. Cone beam computed tomography in craniofacial imaging. Orthod Craniofac Res 2003;6(Suppl 1):31-6.
12. Baba R, Ueda K, Okabe M. Using a flat-panel detector in high resolution cone beam CT for dental imaging. Dentomaxillofac Radiol 2004;33:285-90.
13. Bianchi S, Anglesio S, Castellano S, Rizzi L, Ragona R. Absorbed doses and risk in implant planning: comparison between spiral CT and cone-beam CT. Dentomaxillofac Radiol 2001;30(Suppl 1):S28.
14. Hashimoto K, Arai Y, Iwai K, Araki M, Kawashima S, Terakado M. A comparison of a new limited cone beam computed tomography machine for dental use with a multidetector row helical CT machine. Oral Surg Oral Med Oral Pathol Oral Radiol Endod 2003;95:371-7.
15. Schulze D, Heiland M, Thurmann H, Adam G. Radiation exposure during midfacial imaging using 4- and 16-slice computed tomography, cone beam computed tomography systems and conventional radiography. Dentomaxillofac Radiol 2004;33: 83-6.
16. Ludlow JB, Davies-Ludlow LE, Brooks SL. Dosimetry of two extraoral direct digital imaging devices: NewTom cone beam CT and Orthophos Plus DS panoramic unit. Dentomaxillofac Radiol 2003;32:229-43.
17. Mah JK, Danforth RA, Bumann A, Hatcher D. Radiation absorbed in maxillofacial imaging with a new dental computed tomography device. Oral Surg Oral Med Oral Pathol Oral Radiol Endod 2003;96:508-13.
18. Ziegler CM, Woertcher R, Brief J, Hassfeld S. Clinical indications for digital volume tomography in oral and maxillofacial surgery. Dentomaxillofac Radiol 2002;31:126-30.
19. Nakagawa Y, Kobayashi K, Ishii H, Mishima A, Ishii H, Asada K, et al. Preoperative application of limited cone beam computerized tomography as an assessment tool before minor oral surgery. Int J Oral Maxillofac Surg. 2002;31:322-6.
20. Danforth RA, Peck J, Hall P. Cone beam volume tomography: an imaging option for diagnosis of complex mandibular third molar anatomical relationships. J Calif Dent Assoc 2003;31:847-52.
21. Heiland M, Schmelzle R, Hebecker A, Schulze D. Intra-operative 3D imaging of the facial skeleton using the SIREMOBIL Iso-C3D. Dentomaxillofac Radiol 2004;33:130-2.
22. Hatcher DC, Dial C, Mayorga C. Cone beam CT for presurgical assessment of implant sites. J Calif Dent Assoc 2003;31:825-33.
23. Sarment DP, Sukovic P, Clinthorne N. Accuracy of implant placement with a stereolithographic surgical guide. Int J Oral Maxillofac Implants 2003;18:571-7.
24. Sato S, Arai Y, Shinoda K, Ito K. Clinical application of a new cone-beam computerized tomography system to assess multiple two-dimensional images for the preoperative treatment planning of maxillary implants: case reports. Quintessence Int 2004;35:525-8.
25. Kobayashi K, Shimoda S, Nakagawa Y, Yamamoto A. Accuracy in measurement of distance using limited cone-beam computerized tomography. Int J Oral Maxillofac Implants 2004;19:228-31.
26. Mah JD, Hatcher D. Current status and future needs in craniofacial imaging. Orthod Craniofac Res 2003;6(Suppl 1):10-6.
27. Vannier MW. Craniofacial computed tomography scanning: technology, applications and future trends. Orthod Craniofac Res 2003;6(Suppl 1):23-30.
28. Maki K, Inou N, Takanishi A, Miller AJ. Computer-assisted simulations in orthodontic diagnosis and the application of a new cone beam x-ray computed tomography. Orthod Craniofac Res 2003;6(Suppl 1):95-101.
29. Baumrind S, Carlson S, Beers A, Curry S, Norris K, Boyd RL. Using three-dimensional imaging to assess treatment outcomes in orthodontics: a progress report from the University of the Pacific. Orthod Craniofac Res 2003;6(Suppl 1):132-42.
30. Aboudara CA, Hatcher D, Nielsen IL, Miller A. A three-dimensional evaluation of the upper airway in adolescents. Orthod Craniofac Res 2003;6(Suppl 1):173-8.
31. Danforth RA, Dus I, Mah J. 3-D volume imaging for dentistry: a new dimension. J Calif Dent Assoc 2003;31:817-23.
32. Lascala CA, Panella J, Marques MM. Analysis of the accuracy of linear measurements obtained by cone beam computed tomography (CBCT-NewTom). Dentomaxillofac Radiol 2004;33:291-4.
33. Tsiklakis KK, Syriopoulos K, Stamatakis HC. Radiographic examination of the temporomandibular joint using cone beam computed tomography. Dentomaxillofac Radiol 2004;33:196-201.
34. Beason R, Brooks SL. TMJ imaging accuracy using alpha prototype of DentoCAT cone-beam CT [abstract]. J Dent Res 2004;83(Spec Iss A):1938.
35. Waitzman AA, Posnick JC, Armstrong DC, Pron GE. Craniofacial skeletal measurements based on computed tomography: part I. Accuracy and reproducibility. Cleft Palate Craniofac J 1992;29:112-7.